Diagnostic Accuracy Study

Medicine®

OPEN

Identification of benign and malignant thyroid nodules by in vivo iodine concentration measurement using single-source dual energy CT

A retrospective diagnostic accuracy study

Shun-Yu Gao, MD[a], Xiao-Yan Zhang, PhD[a], Wei Wei, MD[b], Xiao-Ting Li, MD[a], Yan-Ling Li, MD[a], Min Xu, PhD[c], Ying-Shi Sun, MD[a,*], Xiao-Peng Zhang, PhD[a]

Abstract

This study proposed to determine whether in vivo iodine concentration measurement by single-source dual energy (SSDE) CT can improve differentiation between benign and malignant thyroid nodules. In total, 53 patients presenting with thyroid nodules underwent SSDE CT scanning. Iodine concentrations were measured for each nodule and normal thyroid tissue using the GSI-viewer image analysis software. A total of 26 thyroid nodules were malignant in 26 patients and confirmed by surgery; 33 nodules from 27 patients were benign, with 10 confirmed by surgery and others after follow-up. Iodine concentrations with plain CT were significantly lower in malignant than benign nodules (0.47 ± 0.20 vs 1.17 ± 0.38 mg/mL, $P = 0.00$). Receiver operating characteristic (ROC) curve showed an area under the curve (AUC) of 0.93; with a cutoff of 0.67, iodine concentration showed 92.3% sensitivity and 88.5% specificity in diagnosing malignancy. Iodine concentration obtained by enhanced and plain CT were significantly higher in malignant than benign nodules (9.05 ± 3.35 vs 3.46 ± 2.24 mg/mL, $P = 0.00$). ROC curve analysis showed an AUC of 0.93; with a cutoff value of 3.37, iodine concentration displayed 78% sensitivity, 95% specificity in diagnosing malignancy. Combining unenhanced with enhanced iodine concentrations, the diagnostic equation was: $Y = -8.641 \times$ unenhanced iodine concentration $+ 0.663 \times$ iodine concentration. ROC curve showed an AUC of 0.98 (95% CI, 0.94, 1.00). With $Y \geq -2$ considered malignancy, diagnostic sensitivity and specificity were 96%, 96.3%, respectively. This study concluded that SSDE CT can detect the differences in iodine uptake and blood supply between benign and malignant thyroid lesions.

Abbreviations: AUC = area of the curve, FNA = fine needle aspiration, HMW = high molecular weight, HU = Hounsfield unit, NIS = Na(+)/I(–) symporter, ROC curve = receiver operation characteristic curves, ROI = region of interest, SSDE CT = single-source dual energy CT.

Keywords: iodine concentration, single-source dual energy CT, thyroid nodules

1. Introduction

Thyroid cancer is the most commonly diagnosed cancer for Chinese women before the age of 30 years. The largest increase in incidence was seen for thyroid cancers for women from 2000 to 2011, except prostate and cervix cancer.[1] The dramatic rise in thyroid cancer among women is consistent with that observed in other countries.[2–5] Although thyroid cancer is one of the most curable malignancies and only 7% of thyroid nodules are malignant,[6] differential diagnosis cannot be certain.[7,8] The surgical management of benign and malignant thyroid nodules differs substantially. So it is important to diagnose malignancy pre-operatively and to limit unnecessary surgery in the vast majority with benign nodules. Fine needle aspiration (FNA) biopsy is promoted as the tools of choice for diagnosis. But, still with some limitations,[9–13] for example (i) relatively high false-negative rate especially for posterior nodules; (ii) sampling error, because of necrosis in the nodule or the sample cannot represent the whole nodule; (iii) for a patient with multiple nodules in the thyroid gland, FNA biopsy of every nodule is neither cost-effective nor feasible;[7] (iiii) 15% to 30% of FNAs cannot be diagnosed by cytological review with enough certainty.[14]

As well as we know, nodule formation in the thyroid gland can influence iodine uptake and utilization. A study by Doban[15] assessing a large number of samples showed decreased iodine uptake in thyroid cancer cells. Multiple reports have shown that

Editor: Liang Hong.

S-YG and X-YZ contributed equally to this work.

Funding: This work was supported by National Basic Research Program of China (973 Program) (Grant No. 2011CB707705), National Natural Science Foundation of China (Grant No. 81471640), the Capital Health Research and Development of Special Foundation (Grant No. 2011-2015-02), and Beijing Health System High Level Health Technical Personnel Training Plan (No.2013-3-083).

The authors have no conflicts of interest to disclose.

[a] Key laboratory of Carcinogenesis and Translational Research (Ministry of Education), Department of Radiology, [b] Key laboratory of Carcinogenesis and Translational Research (Ministry of Education), Department of Head and Neck Surgery, Peking University Cancer Hospital & Institute, [c] KLMI, Institute of Automation, Chinese Academy of Sciences, Beijing, China.

[*] Correspondence: Ying-Shi Sun, Key laboratory of Carcinogenesis and Translational Research (Ministry of Education), Department of Radiology, Peking University Cancer Hospital & Institute, Beijing, China (e-mail: sys27@163.com).

Medicine (2016) 95:39(e4816)

Received: 7 September 2015 / Received in final form: 15 August 2016 / Accepted: 17 August 2016

http://dx.doi.org/10.1097/MD.0000000000004816

the functional differences between benign and malignant thyroid nodules are associated with Na(+)/I(–) symporter (NIS) protein dysfunction in most thyroid cancer cells.[15–21] Physiologically, thyroid glandular epithelial cells actively transport iodine through the NIS protein for thyroid hormone synthesis. Reduced expression of the NIS gene has been reported in thyroid carcinoma specimens compared with normal thyroid tissues.[21–24] Consequently, NIS was found in higher amounts in normal and benign thyroid tissues compared with malignant tissues. Another study reported decreased NIS expression as the tissues mutated from normal to benign and malignant tissues. All the above data were obtained from resected specimens.

The currently recommended in vivo iodine measurement methods include urinary iodine concentration assessment[25] and thyroid ^{131}I absorption rate determination, both of which only indirectly reflect the iodine concentration with certain limitations; indeed, the effect of dietary iodine can result in iodine measurement inaccuracy. In radiology, Zhang et al[26] attempted to measure CT values of the thyroid gland by using mixed energy CT imaging; afterward, they converted the obtained CT values into iodine concentration, which affects accurate quantitative measurement of iodine concentration.

We wondered whether in vivo measurement of iodine concentration using a noninvasive method could improve the differentiation between benign and malignant thyroid nodules. Indeed, recent technological advances in radiology have made this possible. Single-source dual energy (SSDE) CT is a relatively new CT technique. A generator electronically switches the tube, pulsing rapidly between low energy (80 kVp) and high energy (140 kVp) with each exposure time of 0.5 ms, to produce dual energy images. This scanning mode enables precise registration of data sets for the creation of material decomposition images (e.g., water-based and iodine-based material decomposition images).

The purpose of this study was to determine the value of in vivo iodine concentration measurement in differentiating benign from malignant thyroid nodules by SSDE CT.

2. Materials and methods

2.1. In vitro study

An in vitro experiment was carried out to evaluate the accuracy of iodine concentration measurements. A set of 8 test tubes containing iodine at 0.5 –30.0 mg/mL were scanned by the SSDE CT protocol using fast tube voltage alternating between 80 and 140 kVp with collimation thickness of 0.625 mm, rotation speed of 0.6 s, and helical pitch of 0.983:1. The iodine concentrations were measured using a circular region of interest that covered 80% of the test tube's cross section on the iodine-based material decomposition images. Then, the iodine level measured in each test tube was compared with the known concentration. Finally, a radiologist (**) undertook the quantitative measurements with dedicated imaging viewer (GSI Viewer; GE Healthcare) to analyze the material decomposition images.

2.2. In vivo study

Study population: We retrospectively searched our department's computerized clinical database for all thoracic and cervical SSDE plain and contrast-enhanced CT scanning in which a new abnormality was incidentally identified in the thyroid gland from July 2010 to May 2011. Ethical approval was not necessary. A total of 92 patients were obtained, among which 12 were excluded for diffuse diseases in the thyroid gland (no normal gland found) or with a history of thyroid surgery. A list of patients whose pathologic examination or further imaging and clinical evaluation was scheduled after CT was then extracted. This yielded a final study population of 53 patients (38 women and 15 men) aged 54 ± 9 (range, 38–66) years.

CT protocol: All CT examinations were performed on an SSDE CT scanner (GE Discovery CT750 HD CT scanner; GE Healthcare, Milwaukee, WI) for neck or thorax. The scanner was calibrated regularly with air and water phantom to ensure reliable measurements. Each patient underwent plain and contrast-enhanced CT examinations. Plain CT scanning was carried out in the conventional helical mode after scout CT scanning (tube peak voltage, 120 kVp). Patients were injected with nonionic contrast material via antecubital vein at a rate of 3–4 mL/s (1.5 mL/kg body weight; Omnipaque 300 mg I/mL, GE Healthcare). Other parameters included: collimation thickness, 5 mm; reconstructed thickness, 0.625 mm; tube current, 640 mA; rotation speed, 0.6 s; helical pitch, 1.375; CT dose index volume, 17.65 mGy. The CT images were reconstructed using GSI Viewer. The iodine-based material decomposition images were obtained with pseudo-monochromatic images ranging from 40 to 140 keV.

CT Image Quantitative Analysis: CT images were analyzed by 2 radiologists (** and ** with 5 and 15 years experience in clinical CT, respectively) working together with AW4.4 workstation (GE Medical Systems, Milwaukee, WI) and blinded to the clinical and pathological information. Quantitative analysis of iodine concentration was carried out with GSI Viewer.

ROI drawing: For single isolated nodule, the region of interest (ROI) was placed on its solid regions, avoiding cystic or necrotic regions. For multiple nodules, the ROI was placed on the solid regions of the biggest nodule. For comparison, an additional ROI was placed in the normal thyroid tissue.

Quantitative parameters: Iodine concentrations (mg/mL) in nodules and normal thyroid tissues, respectively, were determined by plain and enhanced CT scanning. Iodine concentrations obtained from plain CT scanning represented the iodine uptake function of the thyroid tissue; Iodine concentration characterized the blood supply in the thyroid tissue.

Iodine concentration = iodine concentration (enhanced CT scanning)-iodine concentration (plain CT scanning).

To ensure consistency, all measurements were done twice at 2-week intervals and mean values were calculated. Prominent artifacts were carefully avoided. For all measurements, the size, shape, and position of the ROI were consistent between the soft-tissue window images and iodine-based material decomposition images as judged by the copy-and-paste function (Fig. 1A and B).

2.3. Clinical and pathological results

The final diagnosis was based on pathological or follow-up information. Thirty-six patients underwent thyroid surgery at our clinic within 1 week after SSDE CT with pathological confirmation. They included 10 patients with benign lesions (4 macrofollicular adenomas, 1 mixed but predominantly macrofollicular adenomas, and 5 adenomatous goiter) and 26 with malignant tumors (25 papillary and 1 follicular carcinomas, respectively).

In total, 17 patients not referred for surgery or FNA biopsy were monitored by clinical and radiological examinations for a median period of 41 months (36–52 months), and no sign of malignancy was observed.

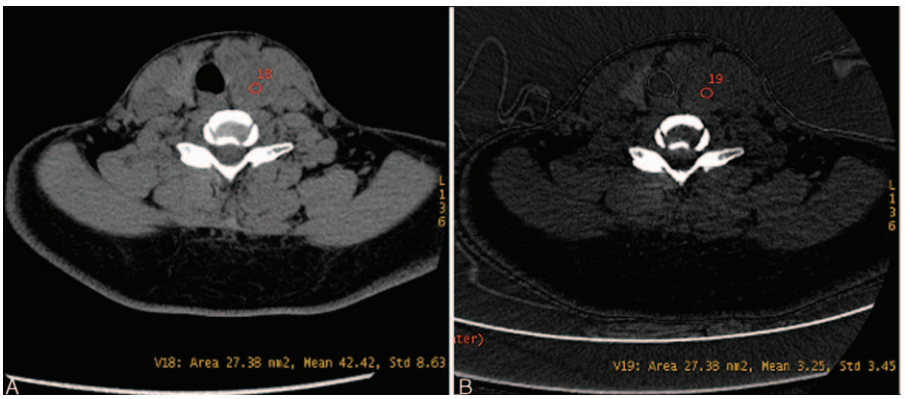

Figure 1. Plain CT image (A) and iodine-base material decomposition map (B), ROI (red circle) in A represent the CT value of the thyroid nodule, ROI (red circle) in B represent the corresponding iodine concentration of the same thyroid nodule. The size, shape, and position of the ROI were consistent between the soft-tissue window images (A) and iodine-based material decomposition images (B) by the copy-and-paste function. CT = computed tomography, ROI = region of interest.

2.4. Statistical analysis

Statistical analysis was carried out with the SPSS software (version 15.0. SPSS Inc). Independent sample *t*-test was used to compare the iodine concentrations between benign and malignant nodules obtained by plain and contrast-enhanced CT scanning. Univariate analysis of variance was done to assess the differences in iodine concentrations between benign nodules, malignant nodules, and normal thyroid gland tissues. The Bonferroni correction was employed for multiple comparisons. Receiver operation characteristic (ROC) curves were generated for iodine concentrations with the Medcalc software (version 11.4.2.0) and area under the curve (AUC) values were determined to assess the overall diagnostic performance in distinguishing between benign and malignant nodules. $P \leq 0.05$ was considered statistically significant.

3. Results

3.1. In vitro study

An excellent correlation was obtained between measured and known iodine concentrations used in the in vitro experiment (Fig. 2 and Table 1).

3.2. In vivo study

3.2.1. Iodine concentration in benign and malignant nodules.

Finally, there were 27 patients with benign nodules and 26 patients with malignant nodules included in the analysis. Iodine concentrations were obtained via material decomposition imaging from plain CT scans. There was no significant difference of iodine concentrations in normal (or uninvolved) thyroid tissues between these 2 groups (benign and malignant nodule groups) ($P = 0.76$). However, statistically significant differences of iodine concentrations were seen among malignant nodules, benign nodules, and normal (or uninvolved) thyroid gland tissues (0.47 ± 0.20, 1.17 ± 0.38, and1.72 ± 0.29 mg/mL, respectively; $F = 155.32$, $P < 0.001$). The ROC curve revealed an AUC of 0.95(0.90–1.00) (Fig. 3A and B) for iodine concentrations obtained by plain CT scanning to evaluate malignant nodules. With the cutoff value set at 0.67 mg/mL, 92.3% sensitivity and 88.5% specificity were obtained for iodine concentration in diagnosing malignancy.

Iodine concentrations were also obtained via material decomposition imaging from enhanced CT scans. There was no significant difference in iodine concentrations of normal thyroid tissues between benign and malignant nodule groups ($P = 0.6$). However, iodine concentrations of 9.05 ± 3.35, 3.46 ± 2.24,

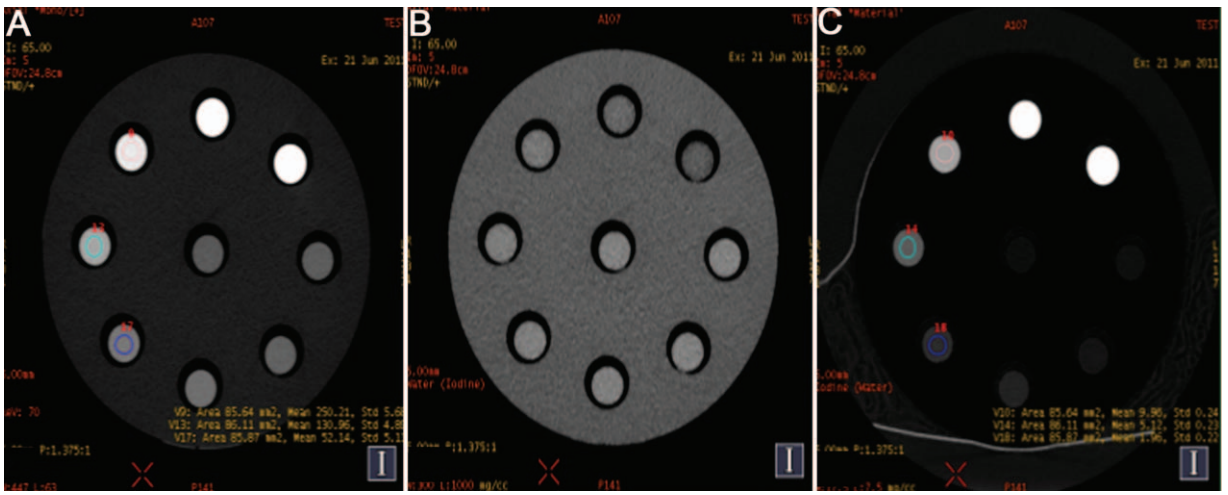

Figure 2. (A) CT image of the phantom contained of different iodine concentrations. (B) The corresponding water-based material-decomposition image. (C) The corresponding iodine-based material-decomposition image. CT = computed tomography.

Table 1

Actual versus measured iodine concentrations at in vitro experiment with SSDE CT.

Actual iodine concentration (mg/mL)	70 keV CT value (HU)	Measured iodine concentration (mg/mL)
30	750.66	30.51
20	492.97	20.02
10	250.21	9.96
5	130.96	5.12
2	52.14	1.96
1	34.90	1.38
0.5	12.30	0.42
0.1	3.74	0.01

HUï¿½=ï¿½Hounsfield unit, SSDE CTï¿½=ï¿½single-source dual energy computed tomography.

and 13.97 ± 3.26 mg/mL were obtained for malignant nodules, benign nodules, and normal thyroid gland tissues, representing statistically significant differences ($F=165.12$, $P=0.00, <0.05$) (Fig. 4A and B). The ROC curve yielded an AUC value of 0.93 (0.82–1.00). With a cutoff value of 3.37, the iodine concentrations showed 78% sensitivity and 95% specificity in diagnosing malignancy.

Combining the unenhanced iodine concentrations and iodine concentrations, the following fitted diagnostic equation was obtained: $Y=-8.641\times$ unenhanced iodine concentration $+0.663\times$ iodine concentrations. This can improve the differentiation between benign and malignant thyroid nodules. ROC curve yielded an AUC of 0.98 (95% CI, 0.94, 1.00) (Fig. 5). $Y \geq -2$ represented malignancy, whereas $Y < -2$ was considered as benignity. In these conditions, diagnostic sensitivity, specificity of 96% and 96.3%, respectively, were obtained.

4. Discussion

Current in vivo iodine measurement methods, including urinary iodine examination and thyroid ^{131}I absorption rate assessment, can indirectly reflect the iodine concentration in the human body, but with limitations such as interference factors, complex preexamination requirements, inaccurate measurement results, and sometimes radiation hazard. Studies have explored the value of CT imaging in iodine measurement. Imanishi et al[27,28] compared the CT values of different thyroid lesions, and found no significant statistical difference. Zhang et al[26] obtained iodine concentrations of thyroid lesions by using the CT value conversion method, and assessing various thyroid lesions, they found no obvious differences in iodine concentrations among different lesions. A series of contradictory results from pathology and basic medical experiments have demonstrated that among different thyroid lesions there are real differences in iodine concentrations, which cannot be detected by conventional CT scanning. We hypothesized that these discrepancies may be due to the mixed energy x-ray used in conventional CT imaging, which result in inaccurate CT value measurement. The mixed energy x-ray CT imaging only reflects the average effect in the mixed energy and cannot be used to further distinguish different materials, for example, in a phenomenon called "different objects with same image characteristics."

Recently a series of papers focused on SSDE CT have demonstrated the usefulness of this new technological advancement in distinguishing one substance from another.[29–33] The fundamentals of physics of SSDE CT mainly states: the substance's absorption capacity varies with changes of x-ray energy, the changes of the absorption capacity of different substances vary with changes of x-ray energy. High-molecular-weight (HMW) substances such as bone and iodine vary a lot with changes of x-ray energy. It is this change with different energy x-ray, which enables further distinction of different substances. This study used the material decomposition technique of the SSDE CT imaging to measure iodine concentrations of the nodule's solid composition and normal thyroid gland tissue. We found overtly higher iodine concentrations in benign nodules compared with malignant ones. Our results were consistent with other reports using basic medical experiments:[15–24] some thyroid follicular cells still existed in adenoma, nodular goiter, and other benign lesions showed normal iodine uptake function; however, thyroid follicular cells were almost totally replaced by cancer cells and fibrotic connective tissues in thyroid papillary carcinoma, which had lost normal iodine uptake function. In our results, the iodine concentration differences detected by SSDE CT were found between benign and malignant thyroid lesions. With a cut-off value of iodine concentration obtained by plain CT scanning set

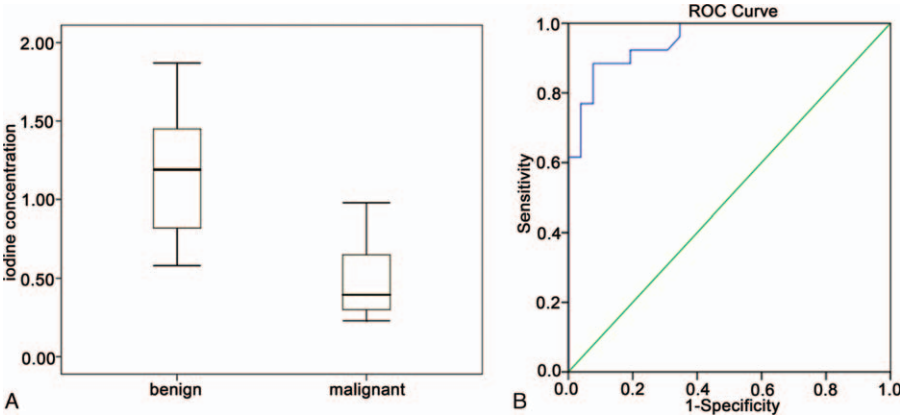

Figure 3. (A) The box plot showed the comparison of iodine concentration (on *Y*-axis) between benign and malignant thyroid nodules (on *X*-axis) obtained by plain CT. (B) The ROC curve (with sensitivity on *Y*-axis and 1-specificity on *X*-axis) showed the diagnostic performance of iodine concentration for assessing malignant nodules. CT = computed tomography, ROC curve = receiver operating characteristic curves.

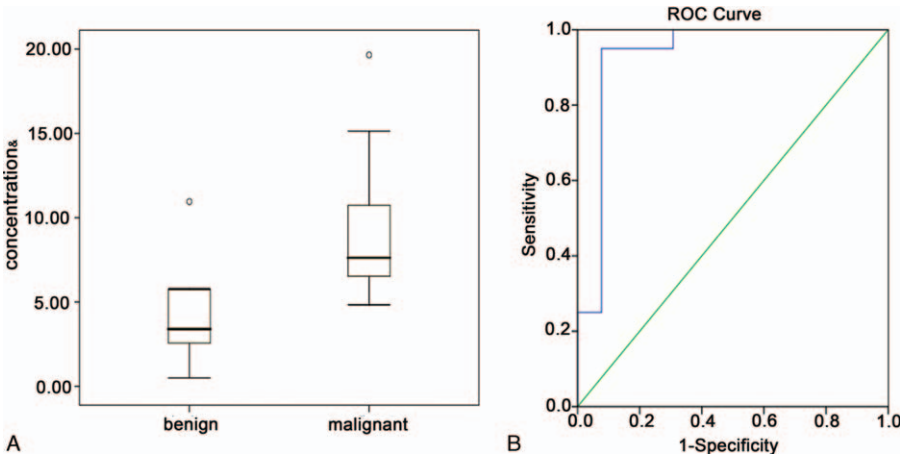

Figure 4. (A) The box plot showed the comparison of iodine concentrations (on *Y*-axis) between benign and malignant thyroid nodules (on *X*-axis) obtained by enhanced CT. (B) The ROC curve (with sensitivity on *Y*-axis and 1-specificity on *X*-axis) showed the diagnostic performance of iodine concentrations for assessing malignant nodules. CT = computed tomography, ROC curve = receiver operating characteristic curves.

at 0.67 mg/mL, 5 cases were misdiagnosed, including 2 cases misdiagnosed as malignancy, and 3 as benign lesions. These data indicated a high sensitivity (92.3%), but a low specificity (88.5%).

It is known that iodine concentrations measured by plain CT scanning reflect the iodine uptake function of thyroid nodules; meanwhile, iodine levels measured by contrast enhanced CT scanning better reflect blood supply of thyroid nodules. In addition, for thyroid nodules with fuzzy boundary or of density difference not so obvious with the surrounding normal thyroid tissues, ROI can be easily obtained by using contrast enhanced CT imaging. Our results showed overtly higher iodine concentrations in malignant thyroid nodules compared with benign nodules after contrast agent injection, in agreement with previous histopathological reports[13,15–22] showing that thyroid carcinoma tissues are rich in blood vessels. Using a cutoff value of 3.37 for iodine concentrations obtained by enhanced CT scanning alone, 7 cases were misdiagnosed as benign lesions, and 1 case as malignancy. These data indicated a low sensitivity (74%), but a high specificity (97%). Considering both sensitivity and specificity, iodine concentrations obtained from plain- and enhanced CT data were assigned different weights to establish a fitting diagnosis equation. Based on this equation, 1 case was misdiagnosed as benign lesion, and 3 cases were misdiagnosed as malignancy. The diagnostic sensitivity and specificity were 96% and 96.2%, respectively. The overall diagnostic accuracy was 96.2%. These data indicate that combining iodine concentrations from plain and iodine concentration from enhanced CT is useful to evaluate the thyroid nodular function and blood supply, providing a better assessment of the thyroid lesion's nature.

In this study, we found an excellent association between the measured and known iodine concentrations in vitro, suggesting the differences in iodine concentrations detected in vivo cannot be attributed to systematic errors. In addition, the iodine concentrations were measured in normal thyroid tissues from the benign and malignant nodule groups, and served as baseline values in this study. No differences were obtained between these groups, indicating that the differences found in the lesions reflect actual characteristics of the lesions and were not the result of systematic errors.

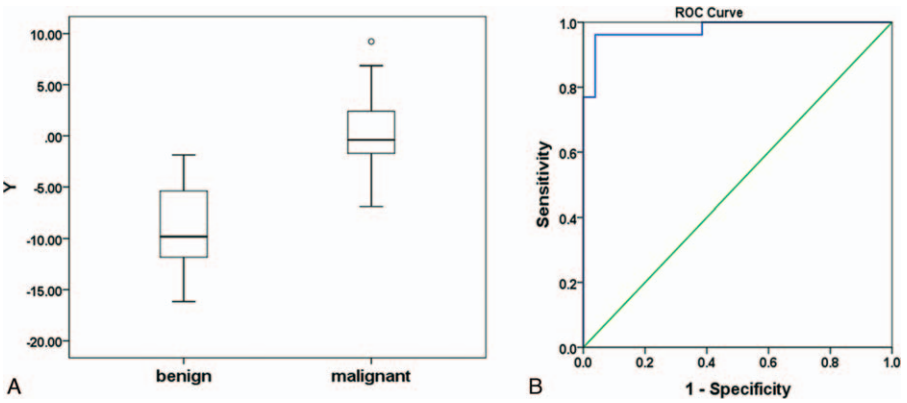

Figure 5. (A) The box plot showed the comparison of *Y* value (on *Y*-axis) between benign and malignant thyroid nodules (on *X*-axis) combining the unenhanced (plain) iodine concentrations and iodine concentrations. (B) The ROC curve (with sensitivity on *Y*-axis and 1-specificity on *X*-axis) showed the diagnostic performance of *Y* value for assessing malignant nodules. $Y = -8.641 \times$ unenhanced iodine concentration $+0.663 \times$ iodine concentrations. ROC curve = receiver operating characteristic curves.

There are some limitations of this study. First, we did not compare the results presented here with those obtained by ultrasound, MRI, or nuclear medicine. Second, in this limited number of patients, most cases of malignant nodules were papillary carcinomas, the most common type of thyroid malignancy, which could bias the analysis. Third, multiple benignancy cases were decided based on clinical data and follow-up; since many thyroid carcinomas are slow growing, no perceptible change might be seen within 3 years or even more. Therefore, the number of benign nodules in this study may be inaccurate. Fourth, the patient population in this study is too small to make a strong case. And as the same reason, we did not do cross-validated analysis for the fitted diagnostic equation. Further studies (more sample size) are therefore required to explore its clinical application. Fifth, the patients in this study received CT scanning due to other tumors or for lymph node evaluation in thyroid cancer patients, the patients did not receive extra or excessive radiation, but in clinical application, we still need to consider carefully avoiding unnecessary radiation.

This study is the first in vivo iodine measurement focusing on thyroid nodules by the material decomposition technology of SSDE CT, which confirmed the feasibility of in vivo iodine measurement. In addition, our conclusions were consistent with known pathological and basic experimental data, indicating the accuracy of in vivo iodine measurement. Therefore, SSDE CT can detect the differences in iodine uptake function and blood supply between benign and malignant thyroid lesions. These findings demonstrate the potential value of SSDE CT imaging to combine anatomical and functional imaging evaluations.

References

[1] Chen Wanqing, Zheng Rongshou, Baade Peter D, et al. Cancer Statistics in China, 2015. CA Cancer J Clin 2016;66:115–32.

[2] Kahn C, Simonella L, Sywak M, et al. Pathways to the diagnosis of thyroid cancer in New South Wales: a population-based cross-sectional study. Cancer Causes Control 2012;23:35–44.

[3] Kilfoy BA, Zheng T, Holford TR, et al. International patterns and trends in thyroid cancer incidence, 1973–2002. Cancer Causes Control 2009;20:525–31.

[4] Morris LG, Sikora AG, Tosteson TD, et al. The increasing incidence of thyroid cancer: the influence of access to care. Thyroid 2013;23:885–91.

[5] Pandeya N, McLeod DS, Balasubramaniam K, et al. Increasing thyroid cancer incidence in Queensland, Australia 1982–2008—true increase or overdiagnosis? Clin Endocrinol (Oxford) 2015;doi: 10.1111/cen.12724. [Epub ahead of print].

[6] Hegedus L. Clinical practice. The thyroid nodule. N Engl J Med 2004;351:1764–71.

[7] Prasad NB, Somervell H, Tufano RP, et al. Identification of genes differentially expressed in benign versus malignant thyroid tumors. Clin Cancer Res 2008;14:3327–37.

[8] Kim JY, Jung SL, Kim MK, et al. Differentiation of benign and malignant thyroid nodules based on the proportion of sponge-like areas on ultrasonography: imaging-pathologic correlation. Ultrasonography 2015;34:304–11.

[9] Ahn SS, Kim EK, Kang DR, et al. Biopsy of thyroid nodules: comparison of three sets of guidelines. Am J Roentgenol 2010;194:31–7.

[10] Misiakos EP, Margari N, Meristoudis C, et al. Cytopathologic diagnosis of fine needle aspiration biopsies of thyroid nodules. World J Clin Cases 2016;16:38–48.

[11] Grewal RK, Ho A, Schöder H. Novel approaches to thyroid cancer treatment and response assessment. Semin Nucl Med 2016;46:109–18.

[12] Ahn SS, Kim EK, Kang DR, et al. Biopsy of thyroid nodules: comparison of three sets of guidelines. AJR Am J Roentgenol 2010;194:31–7.

[13] Kelman AS, Rathan A, Leibowitz J, et al. Thyroid cytology and the risk of malignancy in thyroid nodules: importance of nuclear atypia in indeterminate specimens. Thyroid 2001;11:271–7.

[14] Lebastchi AH, Callender GG. Thyroid cancer. Curr Probl Cancer 2014;38:48–74.

[15] Dohan O, Baloch Z, Banrevi Z, et al. Rapid communication: predominant intracellular overexpression of the Na(+)/I(−) symporter (NIS) in a large sampling of thyroid cancer cases. J Clin Endocrinol Metab 2001;86:2697–700.

[16] Portulano C, Paroder-Belenitsky M, Carrasco N. The Na+/I− symporter (NIS): mechanism and medical impact. Endocr Rev 2014;35:106–49.

[17] Riesco-Eizaguirre G, Rodríguez I, De la Vieja A, et al. The BRAFV600E oncogene induces transforming growth factor beta secretion leading to sodium iodide symporter repression and increased malignancy in thyroid cancer. Cancer Res 2009;69:8317–25.

[18] Galrão AL1, Camargo RY, Friguglietti CU, et al. Hypermethylation of a new distal sodium/iodide symporter (NIS) enhancer (NDE) is associated with reduced NISexpression in thyroid tumors. J Clin Endocrinol Metab 2014;99:E944–52.

[19] Kogai T, Hershman JM, Motomura K, et al. Differential regulation of the human sodium/iodide symporter gene promoter in papillary thyroid carcinoma cell lines and normal thyroid cells. Endocrinology 2001; 142:3369–79.

[20] Liou MJ, Lin JD, Chan EC, et al. Detection of mRNA of sodium iodide symporter in benign and malignant human thyroid tissues. Cancer Lett 2000;160:75–80.

[21] Smanik PA, Ryu KY, Theil KS, et al. Expression, exon-intron organization, and chromosome mapping of the human sodium iodide symporter. Endocrinology 1997;138:3555–8.

[22] Schmutzler C, Winzer R, Meissner-Weigl J, et al. Retinoic acid increases sodium/iodide symporter mRNA levels in human thyroid cancer cell lines and suppresses expression of functional symporter in nontransformed FRTL-5 rat thyroid cells. Biochem Biophys Res Commun 1997; 240:832–8.

[23] Arturi F, Russo D, Schlumberger M, et al. Iodide symporter gene expression in human thyroid tumors. J Clin Endocrinol Metab 1998; 83:2493–6.

[24] Ryu KY, Senokozlieff ME, Smanik PA, et al. Development of reverse transcription-competitive polymerase chain reaction method to quantitate the expression levels of human sodium iodide symporter. Thyroid 1999;9:405–9.

[25] Zimmermann MB. Methods to assess iron and iodine status. Br J Nutr 2008;99(suppl 3):S2–9.

[26] Xin-chuan Zhang, Ji-lin Sun, Qiu-zhi Liu, et al. The research of iodine measurement in thyroid gland by CT and monitoring thyroid diseases lack of. iodine content. China J Control Endemic Dis 1998;13:201–3.

[27] Imanishi Y, Ehara N, Mori J, et al. Measurement of thyroid iodine by CT. J Comput Assist Tomogr 1991;15:287–90.

[28] Imanishi Y, Ehara N, Shinagawa T, et al. Correlation of CT values, iodine concentration, and histological changes in the thyroid. J Comput Assist Tomogr 2000;24:322–6.

[29] Lv P, Lin XZ, Li J, et al. Differentiation of small hepatic hemangioma from small hepatocellular carcinoma: recently introduced spectral CT method. Radiology 2011;259:720–9.

[30] Tijssen MP, Hofman PA, Stadler AA, et al. The role of dual energy CT in differentiating between brain haemorrhage and contrast medium after mechanical revascularisation in acute ischaemic stroke. Eur Radiol 2014;24:834–40.

[31] Liu Y, Qu M, Carter RE, et al. Differentiating calcium oxalate and hydroxyapatite stones in vivo using dual-energy CT and urine supersaturation and pH values. Acad Radiol 2013;20:1521–5.

[32] Ruder TD, Thali Y, Bolliger SA, et al. Material differentiation in forensic radiology with single-source dual-energy computed tomography. Forensic Sci Med Pathol 2013;9:163–9.

[33] Qu M, Jaramillo-Alvarez G, Ramirez-Giraldo JC, et al. Urinary stone differentiation in patients with large body size using dual-energy dual-source computed tomography. Eur Radiol 2013;23:1408–14.